Bioconjugate Chemistry

Article

pubs.acs.org/bc

Sulfonated Polyethylenimine for Photosensitizer Conjugation and Targeting

Upendra Chitgupi,[†] Yumiao Zhang,[†,‡] Chi Y. Lo,[‡] Shuai Shao,[†] Wentao Song,[†] Jumin Geng,[†] Sriram Neelamegham,[†,‡] and Jonathan F. Lovell*[,†,‡]

[†]Department of Biomedical Engineering and [‡]Department of Chemical and Biological Engineering, University at Buffalo, State University of New York, Buffalo, New York 14260, United States

ABSTRACT: Polysulfonated macromolecules are known to bind selectins, adhesion membrane proteins which are broadly implicated in inflammation. Commercially available branched polyethylenimine (PEI) was reacted with chlorosulfonic acid to generate sulfonated PEI with varying degrees of sulfonation. Remaining unreacted amine groups were then used for straightforward conjugation with pyropheophoribide-*a*, a near-infrared photosensitizer. Photosensitizer-labeled sulfonated PEI conjugates inhibited blood coagulation and were demonstrated to specifically bind to cells genetically programmed to overexpress L-selectin (CD62L) or P-selectin (CD62P). In vitro, following targeting, selectin-expressing cells could be destroyed via photodynamic therapy.

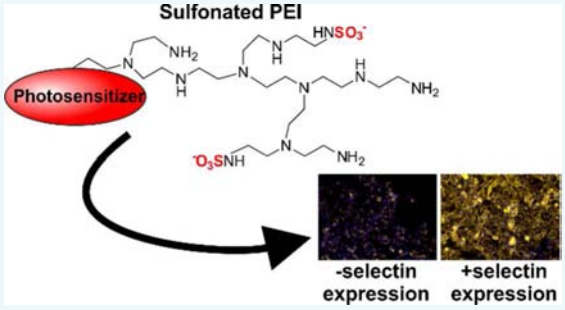

INTRODUCTION

Inflammation plays a central role in numerous chronic conditions that adversely affect health including heart disease,[1] cancer,[2] and metabolic disorders.[3] One of the key steps in inflammatory responses involves the migration and extravasation of leukocytes from blood vessels to the site of insult. This process is mediated by selectins, a family of cell-surface glycoproteins that include endothelial (E-), platelet (P-), and leukocyte (L-) selectin.[4] Selectins contain characteristic extracellular domains that include a (1) calcium-dependent, carbohydrate-binding lectin domain, (2) an epidermal growth factor domain, and (3) a domain consisting of two to nine short consensus repeat units involved in protein binding.[5] Following damage, tissues release cytokines that induce endothelial cells to express E- and P-selectin that in turn bind to circulating leukocytes to induce adhesion to the endothelium. Inflammatory activation by molecules like IL-1β and TNFα increases E-selectin expression over a period of hours, whereas other mediators including thrombin, histamine, and peroxides induce P-selectin expression over a period of minutes.[6]

The binding partners of selectins and their associated biological significance are still being elucidated, but are numerous.[7] One selectin-binding surface protein of interest that is expressed on circulating leukocytes is P-selectin glycoprotein ligand (PSGL-1).[8,9] PSGL-1 contains the tetrasaccharide sialyl-Lewis X (sLe^X) as well as O-linked tyrosine-sulfate residues and these two components together regulate selectin-binding. The unbranched sulfonated heparin glycosaminoglycan, a broadly used anticoagulant, is known to inhibit acute inflammation by reducing L- and P-selectin binding function.[10] Several other sulfonated macromolecules have been reported to interact with selectins to some degree, including fucoidan, dextran sulfate, chondroitin sulfate, as well as other sulfonated lipids and sugars.[11]

Given the importance of selectins in disease, they have become a target in molecular imaging research. P-selectin antibodies have been used to functionalize microbubbles for ultrasound imaging of renal tissue injury[12] and ischemia[13] in mice. Other antibody-based approaches have been used to target E-[14] and L-[15,16] selectins. Theranostic selectin targeting has also been described using selectin-binding peptides,[17,18] aptamers,[19] and sLe^X analogues.[20] One noteworthy synthetic approach involves the use of dendritic polyglycerol sulfate (dPGS) as a platform for L- and P-selectin binding.[21,22] dPGS, which like heparin is a polysulfonated macromolecule, has also been used as a scaffold for fluorescence imaging of inflammation using near-infrared dyes[23,24] and optoacoustic imaging via conjugation to gold nanorods[25] and has the capacity for radiolabeling with synthesis on the kilo scale.[26] However, synthesis of dendrimers can be an intensive process and dPGS itself contains only terminal hydroxyl groups which require further functionalization prior to bioconjugation. Therefore, alternate selectin-binding platforms that are more readily accessible or that are more easily chemically modified could potentially be useful. One candidate includes a derivative of polyethylenimine (PEI), which is abundantly available, contains a large amount of readily modifiable amine groups, and is easily modified to generate sulfonated PEI (s-PEI). s-PEI has been explored in diverse applications related to

Received: April 28, 2015
Revised: May 31, 2015
Published: June 9, 2015

DOI: 10.1021/acs.bioconjchem.5b00241
Bioconjugate Chem. 2015, 26, 1633−1639

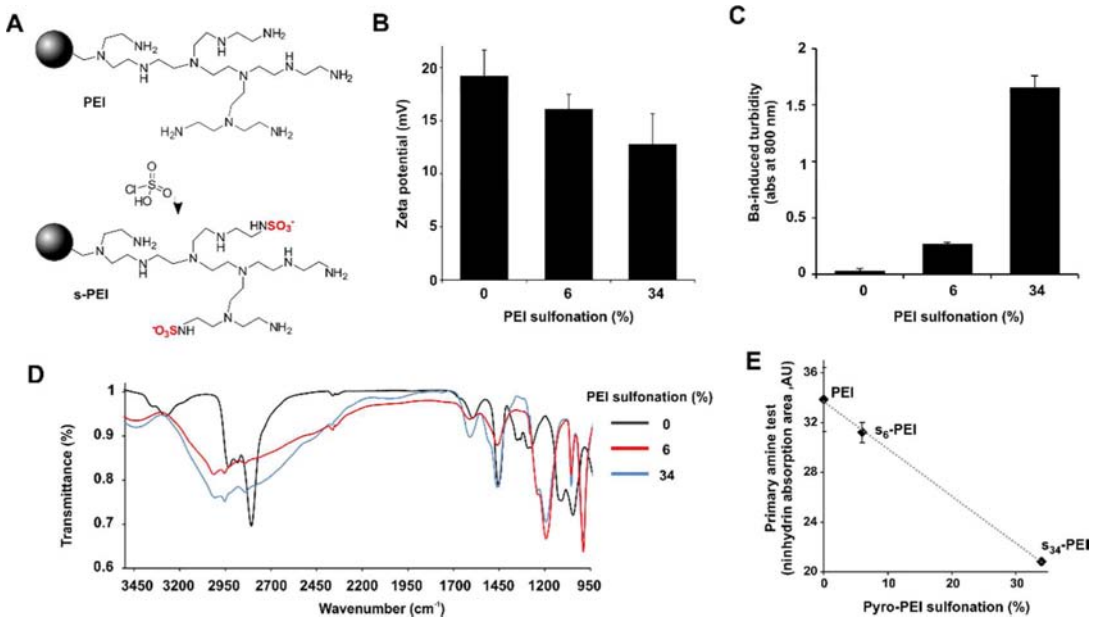

Figure 1. Synthesis and characterization of s-PEI. (A) Reaction of PEI sulfonation. (B) Zeta potential of PEI and s-PEI. (C) Barium chloride turbidity assay for sulfate detection. (D) FTIR spectra of PEI and s-PEI. (E) Ninhydrin test for free amines.

anticoagulants,[27] gene delivery,[28] environmental detoxification,[29,30] and membrane processes.[31]

In this study, we report the synthesis and characterization of s-PEI and subsequent conjugation to the photosensitizer pyropheophorbide-*a* (pyro). Photosensitizers are used in combination with light delivery to target tissues in photodynamic therapy, which is a clinical procedure used to combat various diseases including cancer.[32] Molecular targeting of photosensitizers aims to increase the amount of photosensitizer in the target tissue, thereby reducing harm to nontarget tissues.[33−35] Numerous methods have been explored for photosensitizer targeting including conjugation to antibodies,[36,37] sugars,[38] aptamers,[39] and small molecules.[40] Photosensitizer targeting strategies for cancer typically involve active targeting to cell surface receptors expressed on cancer cells themselves or vascular targeting to tumor blood vessels, either actively or passively.[41] To the best of our knowledge, the development of photosensitizers targeted to selectins has not yet been explored. Since E-selectin is overexpressed in cancers including breast[42] and prostate,[43] selectin-targeted photosensitizers could possibly offer improved tumor selectivity for PDT treatments. Alternatively, as selectin expression has been reported to increase shortly following PDT,[44,45] it might be possible to use PDT to strategically induce selectin expression. This would induce a positive feedback effect in attracting more selectin-targeted photosensitizers to the irradiated tissue. Such an approach could be effective in lowering the total amount of injected photosensitizer, thereby reducing systemic side effects to the patient such as sunlight skin toxicity.

RESULTS AND DISCUSSION

Synthesis and Labeling of Sulfonated Polyethylenimine. Commercially available branched PEI was modified according to published procedures to produce s-PEI with 6% (s_6-PEI) and 34% (s_{34}-PEI) sulfonation.[27] PEI was stirred in methanol at 60 °C with varying amounts of chlorosulfonic acid to generate the s-PEI. Figure 1A shows the chemical reaction, with the bulk of the polymer represented by a sphere and an exemplary segment branch shown. Following the reaction, the product was dissolved in water, precipitated and washed with methanol, and then dried under vacuum to obtain s-PEI. The zeta potential of the s-PEI remained positive, showing that numerous free amine groups remained on the polymer, outweighing the sulfate contribution (Figure 1B). The decrease in zeta potential from +19 mV for the unconjugated PEI to +16 mV for s_6-PEI and +13 mV for s_{34}-PEI was due to the decrease in net positive charge induced by the replacement of cationic amine groups with anionic sulfate residues. A simple and standard analytical test for the presence of sulfate ions involves incubation with barium. This results in an insoluble barium-sulfate complex that can be readily detected by an optical turbidity measurement. We applied this approach to equal concentrations of PEI or s-PEI (10 mg/mL) to confirm the presence of sulfate in s-PEI. As shown in Figure 1C, barium chloride did not induce significant precipitation when added to a solution of standard PEI. However, barium rapidly complexed with s_6-PEI to induce visible aggregation and turbidity in the solution. s_{34}-PEI generated a greater amount of precipitation relative to s_6-PEI. Fourier transform infrared spectroscopy (FTIR) was used to further validate the sulfate group linkages with PEI. Absorption bands at 1190 and 990 cm^{-1} were observed in the s-PEI, but absent in the PEI samples (Figure 1D). These correspond to S═O (asymmetric) and S═O (symmetric) bonds, and the observed bands occurred at wavenumbers close to those previously reported for s-PEI by others.[30] The prominent band appearing close to 2800 cm^{-1} in the PEI sample is attributed to N−H stretching[30] and is weakened in the s-PEI samples. To further confirm the decrease in the number of amine groups due to their conversion to sulfate, we used the ninhydrin assay, which is a common and simple colorimetric method to determine the presence of amines. When ninhydrin was added to solutions of PEI and s-PEI, absorption peaks at 570 nm emerged, which are generated due to the reaction of primary amines with ninhydrin. The peaks were integrated and these values are shown in Figure 1E, as a function of the expected sulfonation degree. An inverse

DOI: 10.1021/acs.bioconjchem.5b00241
Bioconjugate Chem. 2015, 26, 1633−1639

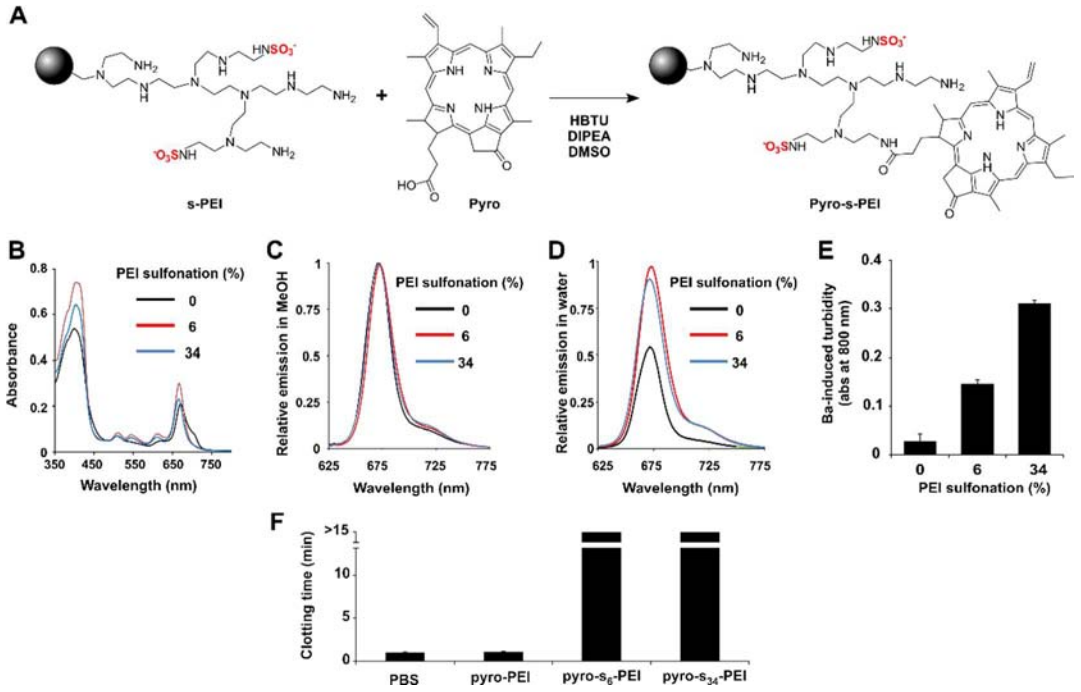

Figure 2. Synthesis and characterization of pyro-s-PEI. (A) Reaction of s-PEI with pyro. (B) Absorption spectra of labeled PEI and s-PEI samples in water following labeling and purification. (C) Fluorescence emission of pyro-labeled samples in methanol, normalized to free pyro in methanol. All samples had equal absorption values at the excitation wavelength of 410 nm. (D) Fluorescence emission of pyro-labeled PEI and s-PEI samples in water, normalized to the maximum emission intensity of free pyro (which was measured in methanol since it has limited water solubility). (E) Barium chloride turbidity assay for sulfate detection of pyro-labeled samples. (F) Blood clotting time of freshly drawn mouse blood immediately incubated with indicated samples (for all PEI samples, the final concentration was 100 μg/mL). Mean ± std dev for triplicate measurements.

linear relationship was observed, suggesting that PEI and s-PEI contained the expected loss of amine groups during their conversion to sulfates. Although the achieved degree of sulfonation was assumed to be consistent with published patent literature,[27] based on the ninhydrin assay to detect a loss in primary amines, the degree of sulfonation was similar to what was expected (7.8% observed vs 6% expected for s_6-PEI and 38.5% observed vs 34% expected for s_{34}-PEI). Additional analysis would be required to more accurately confirm the degree of sulfonation of the samples. Therefore, based on various analytical characterization methods, s-PEI was successfully synthesized and contained available amine groups for further modification.

The photosensitizer pyro, which has a single carboxylic acid group and has been used previously to make targeted photosensitizers,[38] was next conjugated. Pyro was reacted with PEI or s-PEI using a condensation reaction in dimethyl sulfoxide (DMSO) with HBTU as an acid activator and diisopropylethylamine (DIPEA) as a base (Figure 2A). As pyro contains a carboxylic acid group, it could easily react with the amines of PEI and s-PEI to generate pyro-PEI and pyro-s-PEI, respectively. Following the reaction, free pyro was removed by repeated aqueous extraction and then remaining small molecule reactants were removed with dialysis. The resulting conjugates were investigated with spectroscopy. As shown in Figure 2B, there was no shift in the peaks of the absorption profile of the conjugated pyro and pyro effectively labeled both the PEI and s-PEI samples, based on the observed absorption intensities. When the absorption of the samples was adjusted to be equal, all the samples exhibited similar fluorescence when measured in methanol (Figure 2C). However, in water, pyro-PEI exhibited self-quenching compared to pyro-s_6-PEI and pyro-s_{34}-PEI, both of whose brightness was only slightly attenuated compared to free pyro in methanol (Figure 2D). It is possible that the sulfonation inhibited self-quenching in the pyro-PEI samples, which may have been caused by structurally induced pyro dimerization. To verify that pyro-s-PEI retained its sulfate groups during the course of pyro conjugation, the barium turbidity assay was carried out. As expected, with increasing degree of sulfonation, an increased generation in the turbidity was observed, confirming the intactness of the sulfate groups (Figure 2E). When freshly drawn mouse blood was mixed with pyro-s-PEI, but not pyro-PEI, coagulation was effectively inhibited (Figure 2F). Thus, pyro-s-PEI retained the anticoagulatory properties of sulfonated macromolecules.

Cellular Activity of pyro-PEI and pyro-s-PEI. Like many cationic polymers, toxicity concerns are associated with PEI, due to the interactions of large amounts of positive amine groups with cellular structures.[46] The in vitro toxicity of pyro-PEI and pyro-s-PEI was assessed. Cell viability was examined by incubating Chinese hamster ovary (CHO) cells with different concentrations of pyro-conjugated samples (0.4−400 μg/mL) for 90 min and then assessing the viability 24 h later. As shown in Figure 3, following incubation, pyro-s-PEI induced no significant decrease in cellular viability at any of the concentrations examined. However, pyro-PEI significantly inhibited the cellular viability by 50% and 75% at incubation concentrations of 40 and 400 μg/mL, respectively. Therefore, pyro-s-PEI appeared to be less toxic compared to pyro-PEI. These results are consistent with literature examples which have shown that anionic modification of PEI can reduce its cellular toxicity.[47]

Macromolecule sulfonation is important for L- and P-selectin binding,[11] and the vast majority of these sulfate ligands are O-

DOI: 10.1021/acs.bioconjchem.5b00241
Bioconjugate Chem. 2015, 26, 1633−1639

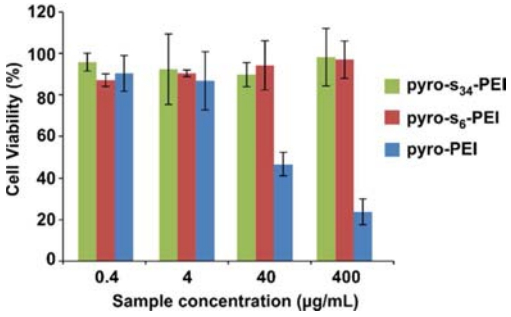

Figure 3. Cell viability of CHO cells incubated with varying concentrations of labeled PEI and s-PEI. Following 90 min incubation, media was replaced and 24 h later viability was assessed using the XTT assay. Mean ± std dev for $n = 3$.

linked groups. However, N-linked sulfates are found (along with O-linked sulfates) on some selectin-binding macromolecules such as heparin. We examined the binding of pyro-s-PEI, which contains N-linked sulfates, to cells overexpressing these selectins. CHO cells were stably transfected with P- and L-selectin as previously described, to generate CHO-P and CHO-L cells, respectively.[48] Pyro-PEI and pyro-s-PEI samples were incubated with all three types of cells for just 3 min at 37 °C, at 100 nM pyro concentration. Following incubation, the cell nuclei were stained with Hoechst dye and the cells were microscopically imaged by examining both the pyro signal and the Hoechst signal (Figure 4). CHO cells exhibited only a relatively weak pyro fluorescence (shown in yellow) when incubated with either pyro-PEI or pyro-s-PEI. However, CHO-P and CHO-L both displayed a prominent pyro signal when incubated with both pyro-s_6-PEI and pyro-s_{34}-PEI, but not nonsulfonated pyro-PEI. This suggests that the pyro-s-PEI samples could rapidly bind to P-selectins and L-selectins expressed on the surface of CHO-P and CHO-L cells, respectively. To further probe the specificity of binding, 50-fold excess unlabeled s-PEI was coincubated with the cells. When excess s-PEI was present, pyro-s-PEI binding was inhibited, suggesting that sulfate interaction to the cells was responsible for the binding.

Given the binding of pyro-s-PEI to cells expressing L- and P-selectin, and that pyro is a photosensitizer, we investigated cell-targeting for photodynamic therapy (PDT) applications. As a control, nonsulfonated pyro-PEI was incubated with CHO, CHO-P, and CHO-L cells, and following irradiation did not induce dramatic PDT cell killing (Figure 5A). Pyro-s_{34}-PEI was incubated with the same cells and then the cells were treated with the same 665 nm irradiation. When pyro-s_{34}-PEI was used, CHO-P and CHO-L were significantly more impacted by the treatment, with 15-fold less viability at a 10 J/cm^2 light dose, compared to CHO cells not expressing selectins (Figure 5B). This demonstrates the in vitro efficacy of pyro-s-PEI as a targeted PDT agent.

CONCLUSION

In summary, s-PEI can readily be generated from commercially available PEI, with varying degrees of sulfonation. s-PEI can then be used for further bioconjugation with photosensitizers to generate materials such a pyro-s-PEI. Pyro-s-PEI was able to specifically bind to cells overexpressing selectins and be used as a selective PDT agent against those cells. Future work includes the application of these chemical compounds in in vivo disease models.

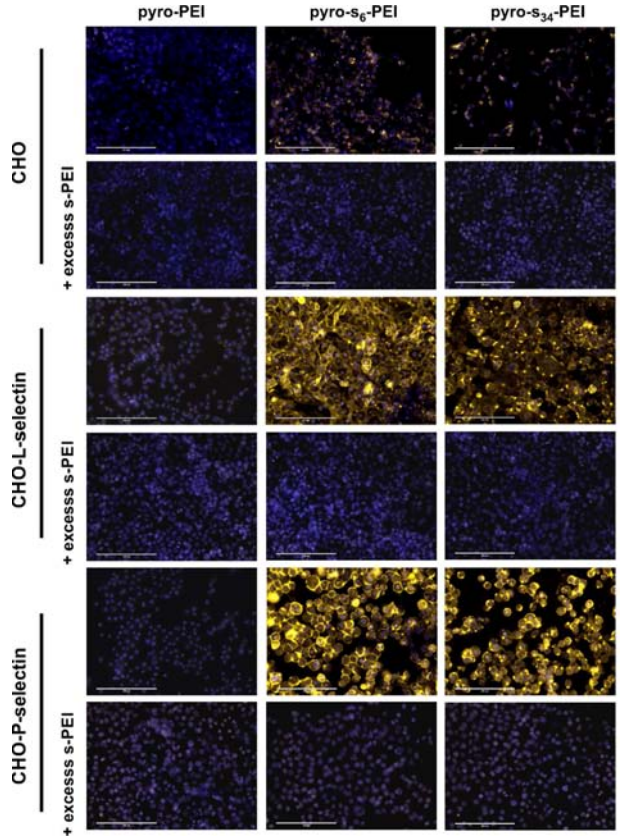

Figure 4. Binding of pyro-s-PEI to selectin-expressing cells. CHO cells expressing the indicated selectins were incubated with pyro-PEI or pyro-s-PEI for 3 min, then were washed and cells visualized with fluorescence microscopy. Pyro is shown in yellow and the nuclear Hoechst stain is shown in blue. Representative results of four separate experiments. 200 μm scale bars are indicated.

EXPERIMENTAL SECTION

Materials. Unless otherwise stated, materials were obtained from Sigma.

Sulfonated-PEI Synthesis. Branched polyethylenimine with a molecular weight of 10 kDa as determined by gel permeation chromatography was obtained from Sigma (# 408727). s-PEI was synthesized as previously reported.[27] In brief, 5 g of PEI was dissolved in 50 mL of methanol and was stirred for 30 min in a three-necked round-bottom flask until PEI was completely dissolved in methanol. Then the solution containing methanol was constantly stirred mechanically and chlorosulfonic acid was added (8.5 mL for 6% and 31 mL for 34%) to the solution. After addition, the solution was heated to 60 °C for 30 min. A thick yellow paste formed, which was then dissolved in 5 mL of water. A precipitate was obtained by adding the aqueous mixture into methanol dropwise. The precipitate at the bottom was washed with methanol twice. This procedure was repeated thrice in order to get a purified product and then it was placed under vacuum for 24 h to obtain s-PEI in powder form. The degree of sulfonation was assumed to be as reported per the patent literature.[27]

Pyro Conjugation. Pyropheophorbide-*a* (pyro) was synthesized as previously reported.[49] s-PEI was dissolved in 1 mL dimethyl sulfoxide (DMSO) via sonication. Subsequently, *O*-benzotriazol-1-yl-tetramethyluronium hexafluorophosphate (HBTU, VWR # 101116−588) was added along with diisopropylethylamine (DIPEA) and pyro, which was also

DOI: 10.1021/acs.bioconjchem.5b00241
Bioconjugate Chem. 2015, 26, 1633−1639

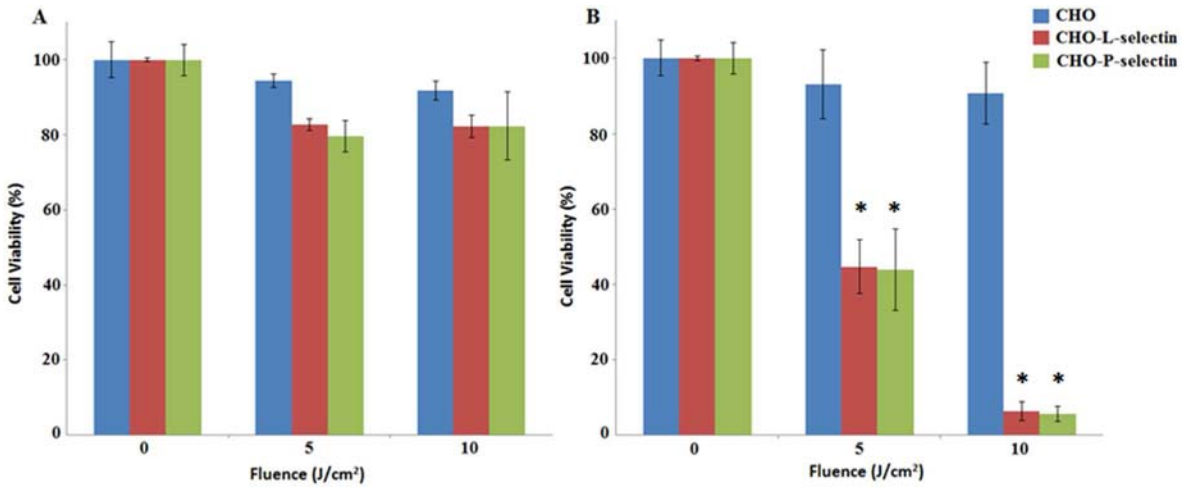

Figure 5. PDT cytotoxicity caused by (A) pyro-PEI and (B) pyro-s_{34}-PEI in CHO cells expressing P- or L-selectin. Pyro-PEI or pyro-s_{34}-PEI was incubated with indicated cells at a concentration of 100 nM pyro in a 96-well plate and then PDT was performed using 665 nm light at the indicated fluences. Cell viability was assessed 24 h later using the XTT assay. Mean ± std dev for $n = 3$. * denotes statistically significant difference ($P < 0.05$) between CHO and CHO-L-selectin or CHO-P-selectin cells based on one-way analysis of variance with post hoc Tukey's test.

dissolved in DMSO. This mixture was magnetically stirred for 24 h after which it was added to water and dichloromethane (DCM) in a 1:1 ratio. The aqueous phase was extracted and this process was repeated thrice to obtain a purified product. Excess solvent and reagents were further removed via membrane-based dialysis with tubing with a molecular weight cutoff of 3.5 kDa (Spectra/Por # S632720) and water was replaced thrice over 12 h.

Polymer Characterization. Fourier transform infrared spectroscopy (FTIR) spectra were collected on Bruker Ram II spectrometer using sulfonated-PEI pellets. Zeta potential was measured with Brookhaven 90Plus PALS instrument in a 10 mM phosphate buffer (pH 7.4). Absorption measurements were recorded on a PerkinElmer Lambda 35 UV/vis spectrometer. Fluorescence measurements were recorded in a Photon Technology International fluorometer.

Primary amines in sulfonated-PEI were quantified by the ninhydrin assay. In short, 5.4 g of sodium acetate was dissolved in 6 mL of deionized water to make a sodium acetate buffer. pH was adjusted to 5.2 using approximately 1 mL of acetic acid and the flask was filled to 10 mL with deionized water. Minutes before the assay, ninhydrin solution was prepared by adding 200 μg of ninhydrin to 7.5 mL of DMSO. Subsequently, 2.5 mL of 4 M acetate buffer was added and then the solution was analyzed. 0.75 mg of PEI/sulfonated-PEI was dissolved in water and 400 μL of this solution was mixed with 300 μL of ninhydrin test solution and heated to 80 °C. The solution was cooled and 400 μL of ethanol was added to the cooled solution. Absorbance of the sample, which obtained a peak at 570 nm was measured and integrated. For the barium chloride assay, 100 mg barium chloride was dissolved in 10 mL deionized water and sonicated until the salt was completely dissolved. Ten mg of PEI or s-PEI was dissolved in 0.5 mL deionized water. 0.5 mL of barium chloride solution was added to 0.5 mL of PEI or s-PEI solution and following 5 min of incubation, the turbidity was measured at 800 nm using a UV/vis spectrometer.

Animal experiments were carried out in accordance with the Institutional Care and Use Committee of University at Buffalo. Clotting activity of blood was measured by incubating the polymer samples with freshly drawn blood of ICR mice. 100 μL of blood was incubated (within few seconds after drawing) with 2 μL of polymer samples for a final polymer concentration of 100 μg/mL and coagulation was observed at 1 min intervals for 15 min.

Cell Viability and PDT. Chinese Hamster Ovary (CHO) cells were cultured at 37 °C (5% CO_2) in Dulbecco's modified eagle's medium (DMEM) supplemented with 10% fetal bovine serum (FBS) and 1% streptomycin/penicillin. CHO cells were seeded in a 96-well plate with 10 000 cells per well. After 24 h, wells were rinsed with PBS (twice) in order to remove the floating cells. Growth medium was replaced with polymer samples of varying concentrations diluted in growth medium followed by a 90 min incubation at 37 °C (5% CO_2). Cells were rinsed with PBS (twice) after incubation and were incubated with 100 μL of fresh media containing serum for 24 h.

For PDT, cell media was replaced with PBS containing pyro-conjugated polymers. The cells were incubated with pyro-PEI and pyro-s_{34}-PEI (pyro concentration: 100 nM) for 3 min and the medium was replaced with 100 μL of fresh media and subsequently treated with 665 nm irradiation at different fluences (0, 5, and 10 J/cm^2). A custom built 665 nm LED-based light box was used for irradiation at a constant fluence rate of 15.3 mW/cm^2. Viability was assessed with XTT after the cells were incubated for another 24 h at 37 °C (5% CO_2).

100 μL of PBS containing 50 μg/mL of XTT (2,3-Bis(2-Methoxy-4-Nitro-5-Sulfophenyl)-2*H*-Tetrazolium-5-Carboxanilide) and 30 μg/mL of PMS (*N*-methyl dibenzopyrazine methyl sulfate) was added to each well and incubated for 3 h. Absorbance values were measured at 450 nm and background values at 630 nm were subtracted from the values at 450 nm at 3 h. To quantify cell viability, cell viability was predefined as the ratio of absorbance of samples with polymer to samples without polymer (control group). Blank XTT values were subtracted from both samples. XTT viability assay was performed in triplicate and standard deviation was calculated based on the triplicate values.

Microscopy. CHO cells (1×10^5) were plated on a 96-well plate in DMEM supplemented with 10% FBS and 1% antibiotics at 37 °C (5% CO_2) and allowed to adhere for 24 h. After washing with PBS twice, the cells were incubated with polymer samples of pyro-PEI or pyro-s-PEI with pyro concentration of 100 nM for 3 min. After washing the samples

DOI: 10.1021/acs.bioconjchem.5b00241
Bioconjugate Chem. 2015, 26, 1633−1639

with PBS twice, nuclei were stained with Hoechst 33342 Fluorescent Stain (100 μL of 7.8 μg/mL) and incubated for 15 min at 37 °C (5% CO_2). The wells were washed with PBS thrice and cells were imaged with an EVOS FL cell imaging system.

AUTHOR INFORMATION

Corresponding Author

*E-mail: jflovell@buffalo.edu.

Notes

The authors declare no competing financial interest.

ACKNOWLEDGMENTS

This work was supported by research funds from the National Institutes of Health (DP5OD017898, HL103411). C.Y.L. was supported by a T32 NIH Ruth L. Kirschstein Postdoctoral Research Training Grant.

REFERENCES

(1) Libby, P., Ridker, P. M., and Maseri, A. (2002) Inflammation and atherosclerosis. *Circulation 105*, 1135−1143.

(2) Coussens, L. M., and Werb, Z. (2002) Inflammation and cancer. *Nature 420*, 860−867.

(3) Hotamisligil, G. S. (2006) Inflammation and metabolic disorders. *Nature 444*, 860−867.

(4) Kansas, G. (1996) Selectins and their ligands: current concepts and controversies. *Blood 88*, 3259−3287.

(5) Tedder, T. F., Steeber, D. A., Chen, A., and Engel, P. (1995) The selectins: vascular adhesion molecules. *FASEB J. 9*, 866−73.

(6) Lasky, L. (1992) Selectins: interpreters of cell-specific carbohydrate information during inflammation. *Science 258*, 964−969.

(7) Varki, A. (1997) Selectin ligands: will the real ones please stand up? *J. Clin. Invest. 99*, 158−162.

(8) Simanek, E. E., McGarvey, G. J., Jablonowski, J. A., and Wong, C.-H. (1998) Selectin−carbohydrate interactions: from natural ligands to designed mimics. *Chem. Rev. 98*, 833−862.

(9) Lo, C. Y., Antonopoulos, A., Gupta, R., Qu, J., Dell, A., Haslam, S. M., and Neelamegham, S. (2013) Competition between core-2 GlcNAc-transferase and ST6GalNAc-transferase regulates the synthesis of the leukocyte selectin ligand on human P-selectin glycoprotein ligand-1. *J. Biol. Chem. 288*, 13974−13987.

(10) Nelson, R. M., Cecconi, O., Roberts, W. G., Aruffo, A., Linhardt, R. J., and Bevilacqua, M. P. (1993) Heparin oligosaccharides bind L- and P-selectin and inhibit acute inflammation. *Blood 82*, 3253−3258.

(11) Varki, A. (1994) Selectin ligands. *Proc. Natl. Acad. Sci. U.S.A. 91*, 7390−7397.

(12) Lindner, J. R., Song, J., Christiansen, J., Klibanov, A. L., Xu, F., and Ley, K. (2001) Ultrasound assessment of inflammation and renal tissue injury with microbubbles targeted to P-selectin. *Circulation 104*, 2107−2112.

(13) Kaufmann, B. A., Lewis, C., Xie, A., Mirza-Mohd, A., and Lindner, J. R. (2007) Detection of recent myocardial ischaemia by molecular imaging of P-selectin with targeted contrast echocardiography. *Eur. Heart J. 28*, 2011−2017.

(14) Reynolds, P. R., Larkman, D. J., Haskard, D. O., Hajnal, J. V., Kennea, N. L., George, A. J. T., and Edwards, A. D. (2006) Detection of vascular expression of E-selectin in vivo with MR imaging. *Radiology 241*, 469−476.

(15) Kang, H. W., Josephson, L., Petrovsky, A., Weissleder, R., and Bogdanov, A. (2002) Magnetic resonance imaging of inducible E-selectin expression in human endothelial cell culture. *Bioconjugate Chem. 13*, 122−127.

(16) Hauff, P., Reinhardt, M., Briel, A., Debus, N., and Schirner, M. (2004) Molecular targeting of lymph nodes with L-selectin ligand-specific US contrast agent: a feasibility study in mice and dogs. *Radiology 231*, 667−673.

(17) Funovics, M., Montet, X., Reynolds, F., Weissleder, R., and Josephson, L. (2005) Nanoparticles for the optical imaging of tumor selectin. *Neoplasia 7*, 904−911.

(18) Jin, A. Y., Tuor, U. I., Rushforth, D., Filfil, R., Kaur, J., Ni, F., Tomanek, B., and Barber, P. A. (2009) Magnetic resonance molecular imaging of post-stroke neuroinflammation with a P-selectin targeted iron oxide nanoparticle. *Contrast Media Mol. Imaging 4*, 305−311.

(19) Mann, A. P., Tanaka, T., Somasunderam, A., Liu, X., Gorenstein, D. G., and Ferrari, M. (2011) E-Selectin-targeted porous silicon particle for nanoparticle delivery to the bone marrow. *Adv. Mater. 23*, H278−H282.

(20) Jubeli, E., Moine, L., Nicolas, V., and Barratt, G. (2012) Preparation of E-selectin-targeting nanoparticles and preliminary in vitro evaluation. *Int. J. Pharm. 426*, 291−301.

(21) Dernedde, J., Rausch, A., Weinhart, M., Enders, S., Tauber, R., Licha, K., Schirner, M., Zügel, U., von Bonin, A., and Haag, R. (2010) Dendritic polyglycerol sulfates as multivalent inhibitors of inflammation. *Proc. Natl. Acad. Sci. U. S. A. 107*, 19679−19684.

(22) Türk, H., Haag, R., and Alban, S. (2004) Dendritic polyglycerol sulfates as new heparin analogues and potent inhibitors of the complement system. *Bioconjugate Chem. 15*, 162−167.

(23) Licha, K., Welker, P., Weinhart, M., Wegner, N., Kern, S., Reichert, S., Gemeinhardt, I., Weissbach, C., Ebert, B., Haag, R., et al. (2011) Fluorescence imaging with multifunctional polyglycerol sulfates: novel polymeric near-IR probes targeting inflammation. *Bioconjugate Chem. 22*, 2453−2460.

(24) Biffi, S., Dal Monego, S., Dullin, C., Garrovo, C., Bosnjak, B., Licha, K., Welker, P., Epstein, M. M., and Alves, F. (2013) Dendritic polyglycerolsulfate near infrared fluorescent (NIRF) dye conjugate for non-invasively monitoring of inflammation in an allergic asthma mouse model. *PLoS One 8*, e57150.

(25) Vonnemann, J., Beziere, N., Böttcher, C., Riese, S. B., Kuehne, C., Dernedde, J., Licha, K., von Schacky, C., Kosanke, Y., Kimm, et al. (2014) Polyglycerolsulfate functionalized gold nanorods as optoacoustic signal nanoamplifiers for in vivo bioimaging of rheumatoid arthritis. *Theranostics 4*, 629−641.

(26) Gröger, D., Paulus, F., Licha, K., Welker, P., Weinhart, M., Holzhausen, C., Mundhenk, L., Gruber, A. D., Abram, U., and Haag, R. (2013) Synthesis and biological evaluation of radio and dye labeled amino functionalized dendritic polyglycerol sulfates as multivalent anti-inflammatory compounds. *Bioconjugate Chem. 24*, 1507−1514.

(27) Murashige, Y., Yanagase, A., Kawachi, Y., and Soga, J. (1987) Sulfonated polyethyleneimine useful as blood anticoagulant. U.S. Patent 4,639,339, January 27, 1987.

(28) Sun, J., Zeng, F., Jian, H., and Wu, S. (2013) Conjugation with betaine: a facile and effective approach to significant improvement of gene delivery properties of PEI. *Biomacromolecules 14*, 728−736.

(29) Leroy, D., Martinot, L., Mignonsin, P., Strivay, D., Weber, G., Jérôme, C., and Jérôme, R. (2003) Complexation of uranyl ions by polypyrrole doped by sulfonated and phosphonated polyethyleneimine. *J. Appl. Polym. Sci. 88*, 352−359.

(30) Saad, D. M. G., Cukrowska, E. M., and Tutu, H. (2012) Sulfonated cross-linked polyethylenimine for selective removal of mercury from aqueous solutions. *Toxicol. Environ. Chem. 94*, 1916−1929.

(31) Shen, L.-Q., Xu, Z.-K., Yang, Q., Sun, H.-L., Wang, S.-Y., and Xu, Y.-Y. (2004) Preparation and characterization of sulfonated polyetherimide/polyetherimide blend membranes. *J. Appl. Polym. Sci. 92*, 1709−1715.

(32) Agostinis, P., Berg, K., Cengel, K. A., Foster, T. H., Girotti, A. W., Gollnick, S. O., Hahn, S. M., Hamblin, M. R., Juzeniene, A., Kessel, D., Korbelik, M., Moan, J., Mroz, P., Nowis, D., Piette, J., Wilson, B. C., and Golab, J. (2011) Photodynamic therapy of cancer: An update. *CA: Cancer J. Clin. 61*, 250−281.

(33) Castano, A. P., Demidova, T. N., and Hamblin, M. R. (2004) Mechanisms in photodynamic therapy: part one—photosensitizers, photochemistry and cellular localization. *Photodiagn. Photodyn. Ther. 1*, 279−293.

DOI: 10.1021/acs.bioconjchem.5b00241
Bioconjugate Chem. 2015, 26, 1633−1639

(34) Solban, N., Rizvi, I., and Hasan, T. (2006) Targeted photodynamic therapy. *Lasers Surg. Med. 38*, 522−531.
(35) Verma, S., Watt, G. M., Mai, Z., and Hasan, T. (2007) Strategies for enhanced photodynamic therapy effects. *Photochem. Photobiol. 83*, 996−1005.
(36) Hudson, R., Carcenac, M., Smith, K., Madden, L., Clarke, O. J., Pelegrin, A., Greenman, J., and Boyle, R. W. (2005) The development and characterisation of porphyrin isothiocyanate-monoclonal antibody conjugates for photoimmunotherapy. *Br. J. Cancer 92*, 1442−1449.
(37) Del Governatore, M., Hamblin, M. R., Shea, C. R., Rizvi, I., Molpus, K. G., Tanabe, K. K., and Hasan, T. (2000) Experimental photoimmunotherapy of hepatic metastases of colorectal cancer with a 17.1A chlorine6 immunoconjugate. *Cancer Res. 60*, 4200−4205.
(38) Zhang, M., Zhang, Z., Blessington, D., Li, H., Busch, T. M., Madrak, V., Miles, J., Chance, B., Glickson, J. D., and Zheng, G. (2003) Pyropheophorbide 2-deoxyglucosamide: a new photosensitizer targeting glucose transporters. *Bioconjugate Chem. 14*, 709−714.
(39) Mallikaratchy, P., Tang, Z., and Tan, W. (2008) Cell specific aptamer−photosensitizer conjugates as a molecular tool in photodynamic therapy. *ChemMedChem 3*, 425−428.
(40) Schneider, R., Schmitt, F., Frochot, C., Fort, Y., Lourette, N., Guillemin, F., Müller, J.-F., and Barberi-Heyob, M. (2005) Design, synthesis, and biological evaluation of folic acid targeted tetraphenylporphyrin as novel photosensitizers for selective photodynamic therapy. *Bioorg. Med. Chem. 13*, 2799−2808.
(41) Chen, B., Pogue, B. W., Hoopes, P. J., and Hasan, T. (2006) Vascular and cellular targeting for photodynamic therapy. *Crit. Rev. Eukaryot. Gene Expr. 16*, 279−306.
(42) Cazet, A., Julien, S., Bobowski, M., Burchell, J., and Delannoy, P. (2010) Tumour-associated carbohydrate antigens in breast cancer. *Breast Cancer Res. 12*, 204−204.
(43) Cai, Y., Wang, J., Li, R., Ayala, G., Ittmann, M., and Liu, M. (2009) GGAP2/PIKE-A directly activates both the Akt and nuclear factor-κB pathways and promotes prostate cancer progression. *Cancer Res. 69*, 819−827.
(44) Evangelou, G., Farrar, M. D., White, R. D., Sorefan, N. B., Wright, K. P., McLean, K., Andrew, S., Watson, R. E., and Rhodes, L. E. (2011) Topical aminolaevulinic acid-photodynamic therapy produces an inflammatory infiltrate but reduces Langerhans cells in healthy human skin in vivo. *Br J. Dermatol. 165*, 513−9.
(45) Gollnick, S. O., Evans, S. S., Baumann, H., Owczarczak, B., Maier, P., Vaughan, L., Wang, W. C., Unger, E., and Henderson, B. W. (2003) Role of cytokines in photodynamic therapy-induced local and systemic inflammation. *Br. J. Cancer 88*, 1772−9.
(46) Lv, H., Zhang, S., Wang, B., Cui, S., and Yan, J. (2006) Toxicity of cationic lipids and cationic polymers in gene delivery. *J. Controlled Release 114*, 100−109.
(47) Zintchenko, A., Philipp, A., Dehshahri, A., and Wagner, E. (2008) Simple modifications of branched PEI lead to highly efficient siRNA carriers with low toxicity. *Bioconjugate Chem. 19*, 1448−1455.
(48) Buffone, A., Mondal, N., Gupta, R., McHugh, K. P., Lau, J. T. Y., and Neelamegham, S. (2013) Silencing α1,3-fucosyltransferases in human leukocytes reveals a role for FUT9 enzyme during E-selectin-mediated cell adhesion. *J. Biol. Chem. 288*, 1620−1633.
(49) Pallenberg, A. J., Dobhal, M. P., and Pandey, R. K. (2004) Efficient synthesis of pyropheophorbide-a and its derivatives. *Org. Process Res. Dev. 8*, 287−290.

DOI: 10.1021/acs.bioconjchem.5b00241
Bioconjugate Chem. 2015, 26, 1633−1639